

Factorization of Numbers with the Temporal Talbot Effect: Optical Implementation by a Sequence of Shaped Ultrashort Pulses

Damien Bigourd,¹ Béatrice Chatel,^{1,*} Wolfgang P. Schleich,² and Bertrand Girard^{1,†}

¹Laboratoire de Collisions, Agrégats, Réactivité, IRSAMC (Université de Toulouse, UPS, CNRS) Toulouse, France

²Institut für Quantenphysik, Universität Ulm, Albert-Einstein-Allee 11, D-89081 Ulm, Germany

(Received 31 August 2007; published 24 January 2008)

We report on the successful operation of an analogue computer designed to factor numbers. Our device relies solely on the interference of classical light and brings together the field of ultrashort laser pulses with number theory. Indeed, the frequency component of the electric field corresponding to a sequence of appropriately shaped femtosecond pulses is determined by a Gauss sum which allows us to find the factors of a number.

DOI: 10.1103/PhysRevLett.100.030202

PACS numbers: 42.65.Re, 02.10.De, 42.79.Kr

In 1836 Henry Fox Talbot used “a magnifying glass of considerable power” [1] to investigate the interference pattern of light emerging from a diffraction grating produced by Joseph von Fraunhofer. Talbot noticed “a curious effect”: the interference patterns in planes parallel to the grating repeated themselves periodically as the distance between the plane and the grating increased. Almost 50 years later this self-imaging effect was rediscovered and explained by Lord Rayleigh [2]. Today the Talbot effect [3] manifests itself not only in electromagnetic waves [4] but also in matter waves with applications ranging from the observation of interferences in C₆₀ molecules [5] to lithography [6]. In this Letter we report on a modern day variant of the Talbot effect using appropriately shaped femtosecond laser pulses and use it to factor numbers.

Factorizing numbers is an important problem in network as well as security systems [7]. Many attempts have been made to use quantum systems to dramatically increase the efficiency. However, even today the challenge remains and only small numbers [8] have been factorized using a quantum algorithm.

At the same time, other physics-based methods for factorizing numbers have been proposed [9]. One of them relies on the properties of the truncated Gauss sum

$$\mathcal{A}_N^{(M)}(l) = \frac{1}{M+1} \sum_{m=0}^M \exp\left(-2\pi i m^2 \frac{N}{l}\right) \quad (1)$$

consisting of $M+1$ terms, and N is the number to be factored. The argument l scans through all integers between 2 and \sqrt{N} for possible factors. When l is not a factor, the quadratic phases oscillate rapidly with m and the sum takes on small values. When l is a factor, then all the phases are multiples of 2π and the sum is equal to unity.

The proposed implementations of $\mathcal{A}_N^{(M)}$ are based on multipath interferences [9]. Each path produces one term in the Gauss sum. The difficulty is to find a system which is experimentally accessible and in which the required phase in Eq. (1) is obtained by a simple variation of a physical parameter.

So far this strict condition has not yet been fulfilled. Nevertheless, several experiments in which each phase of the Gauss sum is separately computed have recently succeeded to demonstrate the ability of Gauss sums to factorize numbers with physical systems. In two experiments based on NMR techniques [10,11] the nuclear spins are driven by a series of radio-frequency pulses. In a more recent experiment, cold atoms are excited by a sequence of Raman π pulses [12].

In the present Letter we introduce an all optical approach toward factoring numbers relying on modern pulse shaping technology. Indeed, the generation of arbitrarily shaped optical waveforms [13] is of great interest in a number of fields ranging from coherent control [14] to information processing [15–17]. For example, pulse shapers have led to an elegant implementation of the Grover search algorithm using Rydberg atoms as quantum registers [15]. Moreover, optical realizations of the Grover [18] or the Bernstein-Vazirani [19,20] algorithms have been used. Our work extends this line of research to factoring numbers using the Talbot effect.

Three elements determine the Talbot effect: (i) a grating which is periodic in space and creates a periodic spatial field distribution, (ii) interference of the waves emerging from each slit of the grating, and (iii) the paraxial approximation of classical optics which leads to the accumulation of quadratic phases in the time evolution of these waves. As a consequence, the intensity distribution of light on a screen is determined by a Gauss sum.

The present implementation follows exactly this recipe except that it takes place in the time rather than the space domain. For this temporal Talbot effect [21], we consider an electric field

$$\tilde{E}(t) = \sum_m w_m e^{i\theta_m} e^{-i\omega_L t} \delta(t - \tau_m) \quad (2)$$

consisting of a sequence of short pulses approximated by delta functions. The pulses of carrier frequency ω_L and phases θ_m appear at times τ_m , and the weight factors w_m guarantee that the energy of the pulse remains finite.

The frequency component

$$E(\omega) = \int_{-\infty}^{\infty} dt \tilde{E}(t) e^{i\omega t} \quad (3)$$

of this pulse sequence defined by the Fourier transform follows from the interference of the Fourier components of the individual pulses

$$E(\Delta\omega) = \sum_m w_m \exp[i(\theta_m + \tau_m \Delta\omega)], \quad (4)$$

with $\Delta\omega = \omega - \omega_L$.

By imprinting appropriate phases on the pulses with pulse shapers we can obtain the quadratic phases characteristic of the Talbot effect. For example, the special choice $\theta_m \equiv -2\pi m^2 N/l$ with times $\tau_m \equiv mT$ and the weight function

$$w_m = \begin{cases} (M+1)^{-1} & \text{for } 0 \leq m \leq M \\ 0 & \text{otherwise} \end{cases} \quad (5)$$

yield for $\Delta\omega = 0$, that is, $\omega = \omega_L$, the Gauss sum Eq. (1). This Gauss sum is thus directly calculated by multipath optical interferences between the optical pulses.

The laser system is a conventional Ti: Sapphire laser delivering pulses of $\tau_L = 30$ fs at 805 nm with 80 MHz repetition rate. The laser pulses are shaped with a programmable 640 pixels phase and amplitude pulse shaper offering a shaping window of $T_w \approx 30$ ps [22].

In order to generate at once the shaped pulse sequence required by Eq. (2), the complex spectral mask

$$H_\theta(\omega) = w_m \sum_{m=0}^M \exp[i(\theta_m + \tau_m \Delta\omega)] \quad (6)$$

is applied with the pulse shaper to modify the Fourier Transform limited input laser pulse: $E_{\text{out}}(\omega) = H_\theta(\omega) E_{\text{in}}(\omega)$. Each term of the sum in Eq. (6) is therefore produced by one ultrashort pulse delayed by τ_m and with an extra phase shift θ_m . Here we choose $T = 200$ fs in order to produce a sequence of well separated pulses.

The interference produced by the pulse sequence is simply analyzed with a high resolution spectrometer. We measure the spectral intensity at the central wavelength $\lambda_L = 2\pi c/\omega_L$ and thus retrieve the Gauss sum for each l . The experiment is performed for l ranging between 2 and \sqrt{N} in order to discriminate factors from nonfactors.

Figure 1 shows two typical spectra obtained for $N = 105$ and $l = 3$ or 9 with $M+1 = 4$ pulses and after averaging over circa 10 s. The complex structure reflects the multipulse interferences and underlines the requested high resolution (about 0.06 nm). The normalization is obtained from full and minimal shaper transmission.

Several numbers have been factorized with this method. In Fig. 2 we display the results of our optical implementation of the factorization scheme based on Gauss sum for $N = 105 = 3 \times 5 \times 7$ obtained with a four-pulse sequence (a), and for $N = 15251 = 101 \times 151$ with a nine-pulse sequence (b). The first example consists of the

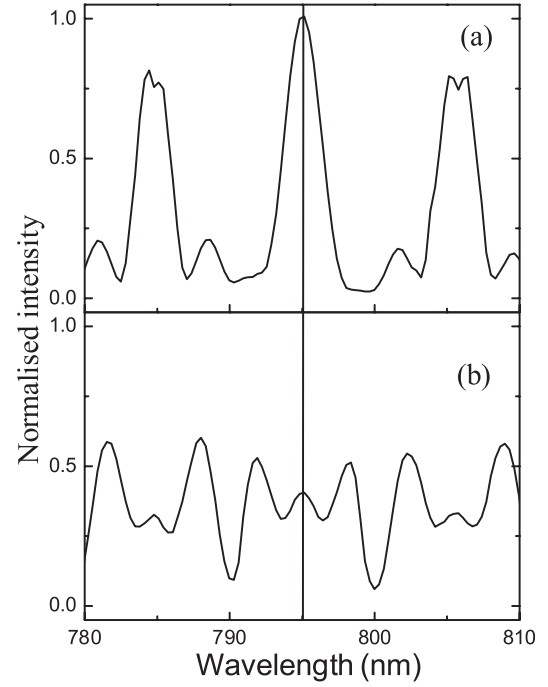


FIG. 1. Spectra of a $M+1 = 4$ pulse sequence ($N = 105$). $l = 3$ (a) and $l = 9$ (b). The vertical line represents ω_L .

product of twin primes whereas the second consist of quite far primes allowing to test the validity of the method.

The experimental data indicated by black dots are compared with the expected values $|\mathcal{A}_N^{(M)}(l)|^2$ depicted by crosses, and the agreement is very good, particularly for the factors whose Gauss sum comes out very clearly. The experimental contrast is in general smaller than expected. This reduction could be due to several experimental limitations. (i) Our shaper is pixilated in the spectral domain and therefore introduces temporal replica. These replica

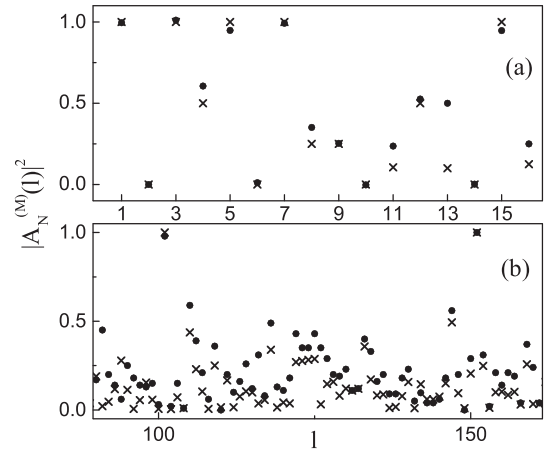


FIG. 2. Experimental realization of factoring using a sequence of shaped ultrashort pulses: (a) $N = 105 = 3 \times 5 \times 7$ with 4 pulses, (b) $N = 15251 = 101 \times 151$ with $M+1 = 9$ pulses. Experiment (dots); theory (crosses).

are separated by 35 ps and are particularly broad and weak due to the nonlinear dispersion in the mask plane [23,24] which was carefully calibrated. This time window of 35 ps is restricted down to 28 ps by the effect of the Gaussian envelope due to the spatial beam profile in the mask plane [22,24]. Its consequences are limited here by working on only a fraction (3–7 ps) of the shaping window. (ii) Another consequence of pixilation is the hole in amplitude associated to large phase steps between consecutive pixels [25] which may induce small distortions as compared to the ideal transmission $H_\theta(\omega)$. (iii) The main limitation to the extinction ratio (currently of 20 dB) is due to the gaps between pixels in the LCD (3% of the pixel width) adding a nonprogrammable pulse at $t = 0$, which participates also to this loss of contrast. This contribution is difficult to compensate and produces undesired interferences with the pulse train [22]. (iv) Finally the resolutions of both pulse shaper and spectrometer limit the ultimate contrast which can be achieved. Both are carefully calibrated following the procedure described in [22].

A key issue in the efficiency and reliability of this scheme is the choice of the truncation parameter M of the Gauss sum. This question is closely related to the phenomenon of ghost factors [26]. Indeed, for certain integer arguments l , the Gauss sum can take values close to unity even when l is not a factor of N . Ghosts can be suppressed [26] below the threshold of $1/\sqrt{2}$ by choosing $M \simeq 0.7\sqrt[4]{N}$.

The example $N = 19043 = p(p + 2)$ with $p = 137$ is perfectly suited to test the predictions of Ref. [26] concerning ghost factors. In this case, N consists of the product of twin primes which are approximately equal and of the order of $\sqrt{N} \cong 137.996$. In this way we can test our method at the upper boundary \sqrt{N} of our set of trial factors. For this purpose we first note that for any integer number N consisting of the product of twin primes the elementary relation $N = p(p + 2) = (p + 1)^2 - 1$ yields the approximation $p + 1 \cong \sqrt{N}$ together with the decomposition $N/(p + 1) = (p + 1) - 1/(p + 1)$. As a result the truncated Gauss sum reduces to

$$\mathcal{A}_{p(p+2)}^{(M)}(p + 1) = \frac{1}{M + 1} \sum_{m=0}^M \exp\left(-2\pi i \frac{m^2}{p + 1}\right). \quad (7)$$

Since $1 \ll M$ and $1 \ll (p + 1)$ we can approximate this sum by a Fresnel integral which yields [26] the scaling $M \propto \sqrt{p + 1} \cong \sqrt[4]{N}$.

In Fig. 3 we display by crosses the exact sum $|\mathcal{A}_{19043}^{(M)}(138)|^2$ as a function of M . We note the slow decay and the oscillations due to the Fresnel integral. Solid dots representing our measurements follow this behavior. The general trend is well reproduced. However, the experimental uncertainties do not allow to reproduce fully the expected oscillations. Moreover, we find the predicted threshold $M \simeq 0.7\sqrt[4]{19043} \simeq 8$. In the inset, an experimen-

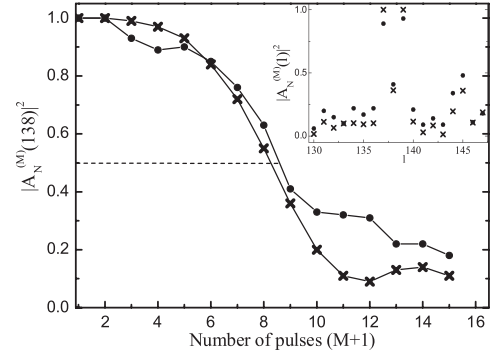


FIG. 3. Suppression of the ghost factor $l = 138$ of $N = 19043 = 137 \times 139$ for increasing number of pulses. Inset : Experimental realization of factoring $N = 19043$ with $M + 1 = 9$ pulses. Experiment (dots); theory (crosses).

tal realization of factoring $N = 19043 = 137 \times 139$ with a nine-pulse sequence is shown as an example. Theory and experiments are also in excellent agreement.

Our work clearly demonstrates that we can use shaped femtosecond pulses to implement Gauss sums and factor numbers. However, many generalizations offer themselves. (i) So far we have only made use of the phases θ_m in the frequency representation Eq. (4) of the electric field. The second contribution to the phase, that is, the product $\tau_m \Delta \omega$, did not enter since we set $\Delta \omega = 0$. (ii) Since we have only the single parameter θ_m at our disposal, the number N to be factored and the trial factor l cannot be varied independently. (iii) Finally we have pursued a sequential rather than a parallel approach. Indeed, we have only used a single spectral component.

The activation of the so far unused phase $\tau_m \Delta \omega$ solves all three problems. Since now we have two parameters we can encode N in τ_m and l in $\Delta \omega$. By recording the complete spectrum we achieve a massive parallelism.

The choice of $\theta_m = 0$ and $\tau_m = 2\pi m^2 N \alpha$ with the numerical constant α also yields the Gauss sum $\mathcal{A}_N^{(M)}$ and illustrates this new approach. Here the spacing between pulses increases quadratically and l is inversely proportional to $\Delta \omega$ such that a single spectrum directly contains all the information.

However, some remaining difficulties need to be overcome: (i) The Gaussian shape of the spectral profile leads to ponderations in the Gauss terms which have to be taken into account. (ii) The variation of l between 2 and \sqrt{N} , i.e., on several orders of magnitudes, puts severe constraints on the spectral resolution necessary to carry the experiment. (iii) Finally, the number of pulses is limited by $\sqrt{T_w}/3\tau_L \simeq 10$ with our present setup.

The quadratic spacing of the pulses required in the above approach might represent a severe problem. The choice $\theta_m = 0$ and $\tau_m \equiv 2\pi(m + m^2/N)$, which leads to the Gauss sum [9]

$$\mathcal{S}_N(\Delta\omega) = \sum_m w_m \exp\left[2\pi i\left(m + \frac{m^2}{N}\right)\Delta\omega\right], \quad (8)$$

might be an interesting way around, since it also allows us to factor numbers. In contrast to the truncated Gauss sum $\mathcal{A}_N^{(M)}$, which only needs to be recorded at integer arguments, the sum \mathcal{S}_N relies on a continuous argument. Here we need the complete spectrum. In return \mathcal{S}_N displays interesting scaling properties which enable us to use the interference pattern for N to factor the number N' by rescaling the frequency axis [27].

We conclude by noting that our implementation is closely connected to the Talbot effect in a harmonic oscillator [28]. Indeed, an initial wave function consisting of an array of sharp maxima located at integer multiples m of a period d accumulates quadratic phases in its time evolution. On first sight this behavior is surprising since the energy spectrum of the harmonic oscillator is linear. However, due to the quadratic dependence of the energy on the position, the maxima at md translate into quadratic phases $(md)^2$. A similar behavior was noted [29] in the quantum carpets woven by a wave packet moving in a harmonic oscillator and consisting only of energy eigenstates with quadratic quantum numbers.

Although the electromagnetic field represents a harmonic oscillator it might be easier to realize a factorization scheme based on this effect using a mechanical oscillator. A laser cooled atom placed into an optical lattice and prepared in its motional ground state offers a possible realization. An absorption grating [30] produced by a standing light wave can prepare the periodic array of narrow wave packets. Moreover, the coupling of the center-of-mass motion to a quantized standing light field [31] can introduce entanglement into the Talbot effect, making factorization with entangled Gauss sums viable.

In summary, we have factorized numbers through the implementation of a Gauss sum with optical interferences produced by a sequence of shaped short laser pulses. This work opens the route to further promising developments based on the wide flexibility offered by optical interferences.

E. Baynard and S. Faure are acknowledged for their technical help. We enjoyed fruitful discussions with G. S. Agarwal, A. Monmayrant, and I. Walmsley. This work has been supported by the Agence Nationale de la Recherche (Contract No. ANR-06-BLAN-0004) and the Del Duca foundation. W. P. S. is grateful to the Max Planck Society and the A. von Humboldt Stiftung for their support. Moreover, he acknowledges the support by the Ministerium für Wissenschaft Forschung und Kunst Baden-Württemberg and the Landesstiftung Baden-Württemberg in the framework of the Quantum Information Highway A8 and the Center for Quantum Engineering.

*Corresponding author.

beatrice@irsamc.ups-tlse.fr

†Also at the Institut Universitaire de France.

- [1] H. F. Talbot, *Philos. Mag.* **9**, 401 (1836).
- [2] L. Rayleigh, *Philos. Mag.* **11**, 196 (1881).
- [3] M. V. Berry, I. Marzoli, and W. Schleich, *Phys. World* **14**, 39 (2001).
- [4] K. Patorski, in *Progress in Optics*, edited by E. Wolf (North-Holland, Amsterdam, 1989), Vol. 28, p. 1.
- [5] B. Brezger *et al.*, *Phys. Rev. Lett.* **88**, 100404 (2002).
- [6] S. Nowak *et al.*, *Opt. Lett.* **22**, 1430 (1997).
- [7] N. Koblitz, *A Course in Number Theory and Cryptography* (Springer, New York, 1994).
- [8] L. M. K. Vandersypen *et al.*, *Nature (London)* **414**, 883 (2001).
- [9] W. Merkel *et al.*, *Fortschr. Phys.* **54**, 856 (2006); *Int. J. Mod. Phys. B* **20**, 1893 (2006); *Phys. Rev. A* **76**, 023417 (2007); J. Clauser *et al.*, *Phys. Rev. A* **53**, 4587 (1996); W. Harter, *Phys. Rev. A* **64**, 012312 (2001).
- [10] M. Mehring *et al.*, *Phys. Rev. Lett.* **98**, 120502 (2007).
- [11] T. S. Mahesh *et al.*, *Phys. Rev. A* **75**, 062303 (2007).
- [12] M. Gilowski *et al.*, preceding Letter, *Phys. Rev. Lett.* **100**, 030201 (2008).
- [13] A. M. Weiner, *Rev. Sci. Instrum.* **71**, 1929 (2000).
- [14] D. Meshulach *et al.*, *Nature (London)* **396**, 239 (1998); N. Dudovich *et al.*, *Phys. Rev. Lett.* **86**, 47 (2001); J. Degert *et al.*, *Phys. Rev. Lett.* **89**, 203003 (2002); B. Chatel *et al.*, *Phys. Rev. A* **68**, 041402 (2003); A. Monmayrant *et al.*, *Phys. Rev. Lett.* **96**, 103002 (2006); *Opt. Lett.* **31**, 410 (2006); *Opt. Commun.* **264**, 256 (2006); A. Assion *et al.*, *Science* **282**, 919 (1998); C. Daniel *et al.*, *Science* **299**, 536 (2003); K. Ohmori *et al.*, *Phys. Rev. Lett.* **91**, 243003 (2003); **96**, 093002 (2006); H. Katsuki *et al.*, *Science* **311**, 1589 (2006).
- [15] J. Ahn *et al.*, *Science* **287**, 463 (2000).
- [16] Z. Zheng *et al.*, *Opt. Lett.* **25**, 984 (2000).
- [17] Z. Amitay *et al.*, *Chem. Phys. Lett.* **359**, 8 (2002).
- [18] N. Bhattacharya *et al.*, *Phys. Rev. Lett.* **88**, 137901 (2002).
- [19] E. Brainis *et al.*, *Phys. Rev. Lett.* **90**, 157902 (2003).
- [20] P. Londero *et al.*, *Phys. Rev. A* **69**, 010302 (2004).
- [21] For an instructive explanation of the temporal Talbot effect see F. Mitschke and U. Morgner, *Opt. Photonics News* **9**, 45 (1998).
- [22] A. Monmayrant *et al.*, *Rev. Sci. Instrum.* **75**, 2668 (2004).
- [23] H. Wang *et al.*, *IEEE J. Sel. Top. Quantum Electron.* **7**, 718 (2001).
- [24] J. Vaughan *et al.*, *Opt. Express* **14**, 1314 (2006).
- [25] W. Wohlleben *et al.*, *Appl. Phys. B* **79**, 435 (2004).
- [26] M. Štefaňák *et al.*, *New J. Phys.* **9**, 370 (2007).
- [27] W. Merkel *et al.* (to be published).
- [28] G. S. Agarwal, *Opt. Commun.* **119**, 30 (1995).
- [29] O. M. Friesch *et al.*, *New J. Phys.* **2**, 4 (2000).
- [30] R. Stützle *et al.*, *Phys. Rev. Lett.* **95**, 110405 (2005).
- [31] For an introduction to atom optics in quantized light fields see W. P. Schleich, *Quantum Optics in Phase Space* (Wiley-VCH, Berlin, 2001), Chap. 20.